Desalination and Water Treatment
www.deswater.com
doi: 10.5004/dwt.2023.30206

316 (2023) 445–451
December

Fabrication of stable and monodispersed magnesium oxide nanoparticles and their reduction potentials

Muhammad Imran Din[a,*], Rida Khalid[a], Zaib Hussain[a], Raafia Noor Afzal[a], Shahbaz Ahmad[b], Safyan Akram Khan[c], Muhammad Younas[d]

[a]*School of Chemistry, University of the Punjab, New Campus Lahore 54590, Pakistan, Mobile No.: +92-33-19743520; Fax: +92-42-99231269; emails: imrandin2007@gmail.com (M.I. Din) ORCID: http://orcid.org/0000-0001-7158-2843, ridakhalid42@gmail.com (R. Khalid), zaib.chem@pu.edu.pk (Z. Hussain), raafianoorafzal@gmail.com (R.N. Afzal)*
[b]*Department of Entomology, Faculty of Agricultural Sciences, New Campus, University of the of Punjab, email: Shahbaz.iags@pu.edu.pk*
[c]*Interdisciplinary Research Center for Hydrogen and Energy Storage. King Fahd University of Petroleum and Minerals Dhahran 31261 Saudi Arabia, email: safyan@kfupm.edu.sa*
[d]*Core Research Facilities, King Fahd University of Petroleum and Minerals, Dhahran 31261, Saudi Arabia, email: muhammad.younas@kfupm.edu.sa*

Received 7 June 2023; Accepted 15 November 2023

ABSTRACT

In this study, a facile green synthesis method was adopted for the fabrication of magnesium oxide nanoparticles (MgO-NPs) from *Calotropis gigantea* (Aak plant) root extract which acted as a capping and reducing agent. The fabricated MgO-NPs were characterized by UV-Vis spectroscopy, Fourier-transform infrared spectroscopy (FTIR) and high resolution-scanning electron microscopy to determine optical, morphological and biological characteristics. UV-Vis spectra results showed an absorption peak at 317 nm whereas scanning electron microscopy showed spherical morphology of the synthesized MgO-NPs. FTIR spectra of the root extract confirmed the presence of phytochemicals, that is, amines, phenols, amides and ketones. Methylene blue (MB) dye was used as model contaminant to assess catalytic reduction potential of the synthesized MgO-NPs. Results obtained showed that biogenic MgO-NPs are suitable for catalytic reduction of MB dye and, when assembled in a sustainable manner, MgO-NPs have the potential to be used for the removal of toxic organic pollutants from industrial effluents.

Keywords: Green synthesis; Nanoparticles; Catalysis; Methylene blue

1. Introduction

Nanoparticles have gained substantial interest because of their microscopic size and large surface-to-volume ratio, the result of which is a substantial shift in their different characteristics including biological, physical, chemical, pharmacological, catalytic, electrical and thermal properties [1,2]. Nanoparticles (NPs) based on metal oxides (MO), notably magnesium oxide (MgO), have been the focus of interest for the past couple of decades because of their peculiar, remarkable and exclusive attributes including low electrical conductivity [3], outstanding refractive index [4], flame-resistance [5], dielectric resistance [6] and higher thermal stability [7] which make them potentially useful in catalysis [8], electrochemical biosensors [9], medical and biomedical applications [4,10], as an antibacterial agent [11] and optoelectronic devices [12]. Over the years, there have been many studies reported on the improvements

* Corresponding author.

that have been made to the fabrication of magnesium oxide nanoparticles (MgO-NPs) due to their outstanding properties and wide range of uses.

Nanomaterial substances have been synthesized by a variety of approaches comprising chemical, physical and even biological applications [13,14]. Physical synthesis employs mechanical forces to split apart massive particles or utilize atom beams in order to produce nanoparticles [15]. Physical vapor deposition (PVD), mechanical milling and sputtering are the commonly employed physical methods [16–18] for the biosynthesis of nanoparticles. The physical approaches were accomplished under tough working conditions and with energy-intensive experimental setup [19]. The chemical synthesis of NPs involves the generation of ions through a series of chemical processes. Chemical vapor deposition (CVD), liquid phase method, sol–gel, co-precipitation, hydrothermal, colloidal method, reduction method and electrodeposition (ED) are some of the usually employed chemical methods for NPs synthesis [20–24] but synthesis using chemical pathways required the use of toxic organic solvents and harmful reducing agents, which produced undesired intermediates that had a severe effect on the surrounding ecosystem [25,26]. Due to the drawbacks associated with chemical and physical procedures, researchers are looking towards biological approaches as a viable alternative.

One biosynthesis strategy for nanoparticles which helps eliminate hazardous byproducts, and is engaged in optimizing nanoparticle diameter, is plant extract assisted synthesis [27,28]. The existence of phytochemicals in plants, which function as both a reducing agent and a stabilizing agent, is a crucial factor which contributes to the acceleration of the production of nanoparticles. For the creation of metal oxide nanoparticles, phytocomponents such as polyphenols (phenolic acid, flavonoids and terpenoids), organic acids and proteins are being studied as potential bio-reducing and stabilizing agents [29,30]. Many researchers estimate that plant extracts, because of the high number of phytochemicals that are included in them, have the potential to accelerate the production of metal oxide nanoparticles [31,32]. Abdallah et al. [33] reported plant-mediated biosynthesis of MgO nano-flowers (MgO NFs) having <20 nm in size which exhibited potent antibacterial activity against the pathogen Xoo (rice bacterial blight). These NFs were synthesized using rosemary (*Rosmarinus officinalis* L.) which exhibits strong antibacterial properties. Ogunyemi et al. [34] fabricated magnesium oxide (MgO) and manganese dioxide (MnO) nanoparticles using *Matricaria chamomilla* L. extract and used it as an alternate management strategy to counter bacterial brown stripe (BBS) condition by immersing rice seedlings in the solution of bio-fabricated nanoparticles.

Therefore, the purpose of this study was to find solutions to the numerous issues that are caused by the traditional methods that are applied throughout the manufacturing process of nanomaterials. The extract of *Calotropis gigantea* (Aak plant) roots was used for this purpose, rather than potentially damaging supportive media and reducing agents. *C. gigantea* Linn belonging to the family Asclepiadaceae, is a well-known medicinal herb having phytochemical components flavonoids, tannins, saponins, phenolic compounds and alkaloids. All parts (roots, leaves, flowers and stem) of the plant are used in the treatment of different diseases including bronchitis, asthma, gastrointestinal irritation, joints pain, swelling and tooth decay. In particular, roots are utilized in the treatment of lupus, tuberculous leprosy as well as syphilitic ulcers [35–38]. Some other applications include use as biofuel, bio pesticides, surfactant and as a dehairing agent of leather [39–41]. Owing to its high antioxidant potential, which makes it an effective reducing as well as stabilizing agent for the synthesis of metal oxide NPs, a number of different studies have been conducted on the extract of various parts of the *C. gigantea* plant including the leaves, flowers and latex. These studies have been done in order to produce a variety of MO-NPs [42]. Till date, no data has been published on the utilization of *C. gigantea* root extract in the production of MgO-NPs. In addition to this, MgO-NPs application in the catalytic reduction of methylene blue (MB) dye was also studied.

2. Materials and methods

C. gigantea was obtained from the local vicinity of Lahore City, Pakistan. All chemicals used were of analytical grade and obtained from Sigma-Aldrich. No further treatment or purification was carried out. Magnesium nitrate hexahydrate [$Mg(NO_3)_2{\cdot}6H_2O$] was used as a precursor salt for MgO-NPs synthesis along with distilled water (H_2O). Other chemicals used include sodium borohydride ($NaBH_4$) and sodium hydroxide (NaOH).

2.1. Preparation of C. gigantea root extract

To prepare the root extract solution for *C. gigantea* plant, the roots were first washed with tap water and then thrice in distilled water to remove any remaining dirt. Further, the roots were ground to make root powder after which 15 g of root powder was dissolved in 100 mL diluted water. The solution was boiled at 80°C for 3 h. In order to purify the root extract, filtration was carried out using Whatman filter paper. Appearance of a yellowish hue was observed in the aqueous solution. Thus, an aqueous root extract solution using *C. gigantea* plant, which serves as a capping and reducing agent, was formed.

2.2. Preparation of MgO-NPs

In the process of MgO-NPs synthesis, a beaker containing 20 mL of a solution containing 1 M $Mg(NO_3)_2{\cdot}6H_2O$ was combined with 20 mL of root extract solution using microwave assisted method. The solution was stirred continuously on a hot plate with magnetic stirrer at 90°C for 120 min. The solution started to form a yellowish-brown color indicating that the Mg-salt precursor was being converted into MgO-NPs. The solution was then centrifuged for 10–15 min at 45,000 rpm in a centrifugation machine and then analysed using Fourier-transform infrared spectroscopy (FTIR) and UV/Vis spectroscopy to determine fabrication of the MgO-NPs. After multiple washings of the centrifuged solution in distilled water followed by filtration, the obtained precipitates were dried in an oven for 1 h before being calcined in a muffle furnace at a temperature of 400°C for 2 h. Fine powdered MgO-NPs were

obtained by grinding in a pestle and mortar and then stored in airtight sample vials for further use.

2.3. Characterization of synthesized MgO-NPs

C. gigantea root extract was effectively used to generate MgO-NPs by acting as a capping and reducing agent. The optical, morphological and biological characteristics of the MgO-NPs under study were analyzed.

2.3.1. Fourier-transform infrared spectroscopy

In this study, FTIR spectra obtained in the range of 400–4,500 cm^{-1} was used to determine the chemical constituent and functional group present in the MgO-NPs under study.

2.3.2. UV-Visible spectroscopy

UV-Vis spectroscopy was used to record the optical characteristics of the nanoparticles. Utilizing UV-Visible spectroscopy, it was possible to determine the properties of MgO-NPs that were produced by reducing Mg ions. The synthesized MgO-NPs were initially characterized using a double beam LAMBDA-3500 UV-Visible spectrophotometer with a resolution of 0.1 nm.

2.3.3. Scanning electron microscopy

Scanning electron microscopy (SEM) analysis enabled visualization of the surface morphology of the studied MgO-NPs. Prior to analysis the sample was dried for 5 h at 100°C. To investigate the morphological peculiarities of the synthesized MgO-NPs, high resolution-scanning electron microscopy at 25 kV was employed.

2.4. Catalytic reduction

Double beam UV-Vis spectrophotometer was employed to analyze the catalytic reduction of MB dye. MB dye solution (1.5 mL), 6 mM $NaBH_4$ solution (0.6 mL) and 0.1 mg/mL (0.4 mL) MgO-NPs were mixed together and placed in a 2.5 mL quartz cuvette. A range from 260 to 760 nm was chosen as the acceptable values for the wavelengths. UV spectra were continuously scanned while monitoring the procedure until the absorbance level stabilized. The intense blue color of the MB dye solution started to fade away thus becoming colorless hence confirming the reaction was complete. The color and absorption strength of the solution were monitored in real time using UV-Vis spectrometer. Catalytic degradation of the MB dye solution was expressed as a percentage:

$$\%D = \frac{A_o - A_t}{A_o} \times 100 \quad (1)$$

where A_0 = Initial concentration and A_t = Final concentration

3. Results and discussion

3.1. UV-Vis analysis

The most common method for monitoring the properties of NPs is performed using ultraviolet–visible (UV/Vis) spectroscopy [43]. The successful synthesis of MgO-NPs was confirmed by the appearance of an absorption peak at 314 nm for the particles analysed prior to calcination (Fig. 1). This gives evidence for the reduction of $Mg(NO_3)_2$ as well as the appearance MgO-NPs. In most cases, the featured peak produced for MgO-NPs under UV/Vis can be found between 280 and 400 nm. After the nanoparticles had been synthesized they were calcined and an absorption peak at 317 nm was measured. The fact that the peak location moved very slightly in either direction indicates that the calcination procedure altered the properties of the NPs. It is possible that the shifting of this peak position in the UV spectrum can be attributed to the calcination process which removes the capping agent from the NPs. Furthermore, a longer calcination time may result in larger nanoparticles in addition to the creation of crystals of varying sizes [44,45]. The data that have been presented is consistent with that reported by Almontasser et al. [46] with λ_{max} at 380 nm.

3.2. FTIR analysis

The FTIR spectra of plant-mediated MgO-NPs is shown in Fig. 2. FTIR spectroscopic analysis was used to explore the chemical changes that may have taken place during the formation of MgO-NPs. Phenol, ethanol, amino acids, alkanes, alkynes and carboxylic acids were all identified in the root extract using FTIR. Based on these structural motifs, it can be inferred that the root extract contains alkaloids, flavonoids, polyphenols, terpenes and terpenoids. Fig. 2a shows FTIR spectra of root extract. The obtained broad band at 3,237–3,465 cm^{-1} refers to O–H group stretching. The absorption value at 1,530 cm^{-1} indicates the presence of an aromatic ring. Broad bands at 3,380; 2,123 and 1,530 cm^{-1} show the presence of hydroxyl group (–OH), aldehydes group, aromatic and amines ring, respectively. Multiple published investigations have shown that peaks at the 724 cm^{-1} position for MgO can be seen between the range of 500 and 800 cm^{-1}, proving that MgO-NPs were successfully synthesized (Fig. 2b). Pugazhendhi et al. [47] used an aqueous extract of the brown algae *Sargassum wightii* to

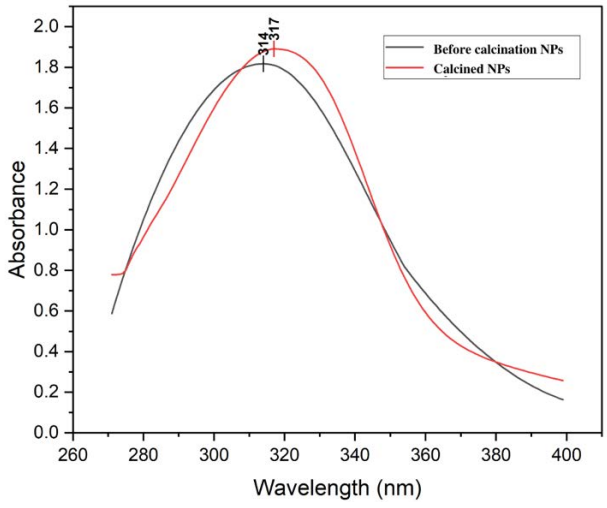

Fig. 1. UV-Vis spectrum of plant mediated MgO-NPs.

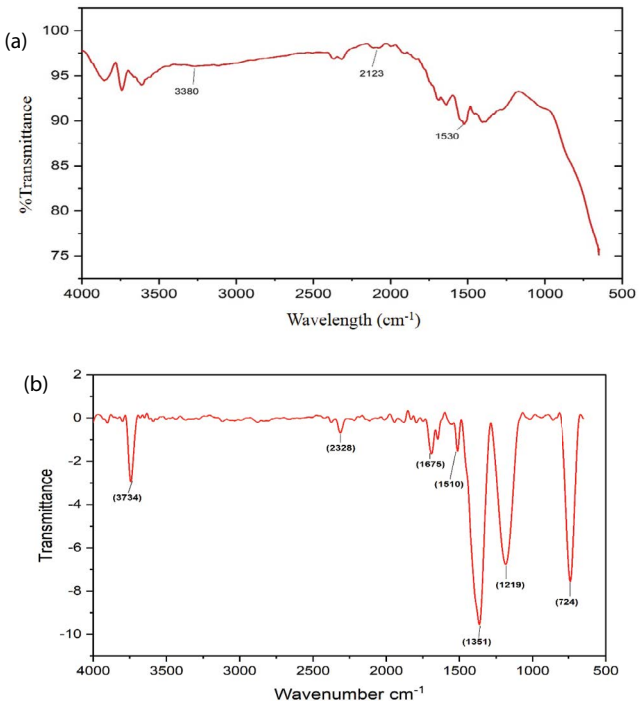

Fig. 2. Fourier-transform infrared spectroscopy analysis of (a) Aak plant root extract and (b) synthesized MgO-NPs using Aak plant root extract.

biosynthesize MgO-NPs. The study of an absorption maximum between 660 and 540 cm^{-1}, which suggests Mg–O bond stretching, validated the synthesis of MgO-NPs. Research into its photocatalytic, anticancer and antibacterial properties was also conducted. Fouda et al. [48] reported that MgO-NPs can be synthesized by using environmentally friendly methods, as evidenced by the presence of a stretching band at 437–677 cm^{-1}. Biosynthesized MgO-NPs have been shown to be useful for photocatalytic reductions of tannery effluent and elimination of hazardous environmental contaminants from textile colors. O–H stretching vibrations are responsible for the 3,734 cm^{-1} band, whereas the weaker bands at 1,675 and 1,510 cm^{-1} are attributable to C–H bending vibrations. C=O, C–O stretching and S=O stretching are all possible explanations for the peaks at 2,328; 1,219 and 1,351 cm^{-1}, respectively.

3.3. SEM analysis

The scanning electron micrograph of the synthesized MgO-NPs generated under optimal conditions and having a size scale of 10 μm (1,000 nm) can be seen in Fig. 3. The topological examination of the nanostructures revealed that they had a spherical morphology and their average size was found to be less than 100 nm. Agglomeration was also seen in some locations as shown by a few large clusters that can be seen in the SEM image. This phenomenon can be explained by the synthetic route that was taken and the biological inhibition competence of the phytochemicals that were found in the plant extract. Another reason is that the electrostatic attraction and polarity of magnesium NPs led to some agglomeration of the produced nanoparticles,

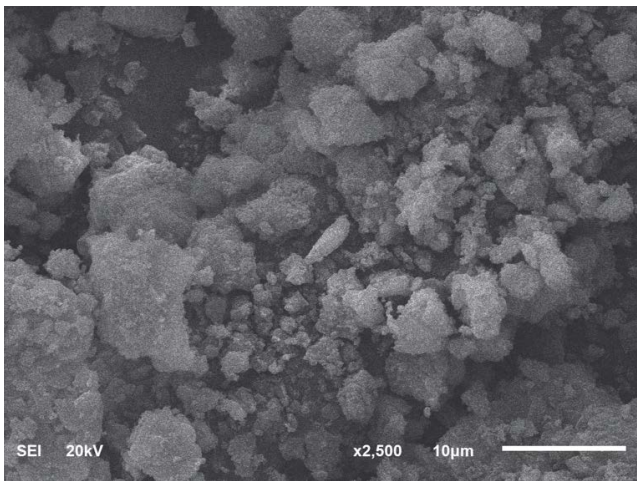

Fig. 3. Scanning electron microscopy image of magnesium NPs.

which can be seen in the image. In these SEM images, the surface morphologies resembled clusters of spherical nanoparticles. The obtained results can be closely related to the data available in literature. Suresh et al. [49] highlighted that SEM photographs of the obtained magnesium nanoparticles showed that the prepared powders contained a combination of fine and coarse granules of the product particles. Smaller grains of irregular size were seen in certain samples while larger particles were more noticeable in others. Based on scanning electron micrographs, the average size of nanoparticles was between 60 and 70 nm. The topological examination of the nanostructures carried out by Khan et al. [4] revealed that they had a spherical morphology and their average size was found to be less than 50 nm. Agglomeration was also seen in certain locations, which was denoted by a few large clusters.

3.4. Catalytic reduction of MB dye

In this part of the study, feasibility of employing MgO-NPs as a catalytic degrading agent for MB with $NaBH_4$ as a reductant is explored. Reducing methylene blue catalytically is crucial because it is highly hazardous yet its reduction product is safe and environmentally sustainable. The degradation of MB dye with $NaBH_4$ is only thermodynamically feasible but not kinetically. Hence, efficient MgO-NPs catalyst has been used in basic medium to evaluate the reduction of MB dye. The MgO-NPs work efficiently with $NaBH_4$ along with MB. For the catalytic reduction pathway to work, both the contaminant molecules and the BH_4^{-1} ions must be brought to the surface of the MgO-NPs (Fig. 4). The borohydride ion aids in transfer of electrons on the MgO surface which results in formation of hydride ions. These hydride ions further react with protons to form molecular hydrogen [Eq. (2)]. The MgO catalyst provides an electron from its conduction band which aids in generation of active hydrogen from molecular hydrogen [Eq. (3)]. The generated hydrogen further reacts with MB dye and degrades it into leuco-methylene blue. However, as the reaction continues, the blue color of the dye diminishes and eventually disappears, leaving behind a colorless residue. When the chemical reaction is

complete, resulting products diffuse away from the catalysts site and into the surrounding bulk material [50,51].

$$NaBH_4 + H_2O \rightarrow NaBO_4 + H_2 \quad (2)$$

$$MgONPs + H_2 \rightarrow H - MgONPs - H \quad (3)$$

Using a double beam spectrophotometer, the degradation was monitored by taking absorbance measurements at 664 nm at 1.5 min intervals. Fig. 5 shows that the degradation of MB was completed in 30 min in the presence of MgO-NPs catalyst.

A graph depicting how absorbance changed with time is illustrated in Fig. 6a and b. This allowed the reaction rate to be determined using the Beer–Lambert law, which compares the absorbance of a reactant molecules at a given characteristic time (t) to its absorption at the beginning of the experiment (A_t/A_0), where (A_t/A_0) is proportional to the concentration of the reactant molecules at the beginning of the experiment (C_t/C_o). Success in removing MB dye was shown by a gradual and linear decrease in $\ln(A_t/A_0)$ values over time.

Research has shown that the catalytic reduction of MB, like the reduction of many other aromatic pollutants, appears to generally obey first-order kinetics. This section presents the fundamental equation of first-order kinetics:

$$k_{app}(\text{dye}) = -\frac{d(\text{dye})}{dt} \quad (4)$$

3.5. Stability of MgO-NPs catalyst

Every catalyst's recyclability demonstrates its stability, durability, market sale and sustainability. A stable catalyst maintains its activity even after several cycles of recycling [52]. To check the efficiency of biogenic synthesized MgO-NPs catalyst, MB was selected as a model pollutant. For this purpose, the MgO-NPs were separated, washed and dried in an oven. The MgO-NPs catalyst was then re-dispersed in water for further reaction. The percentage activity (%) of MgO-NPs was calculated using Eq. (5).

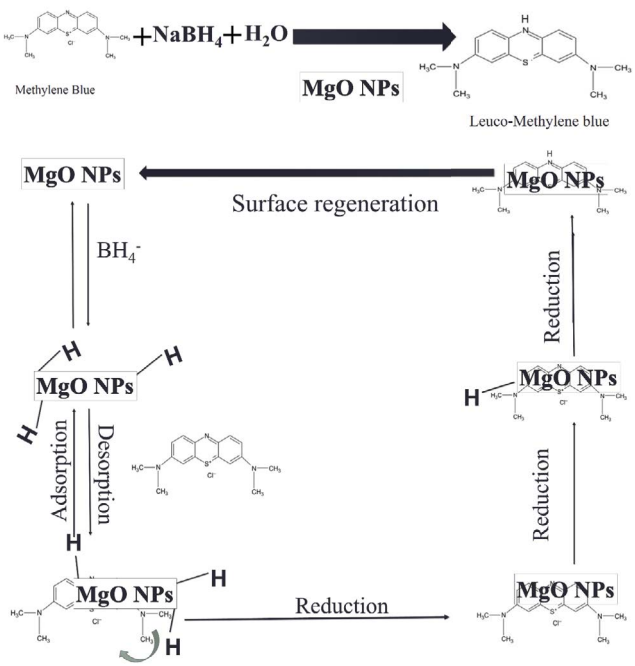

Fig. 4. Catalytic reduction mechanism of methylene blue.

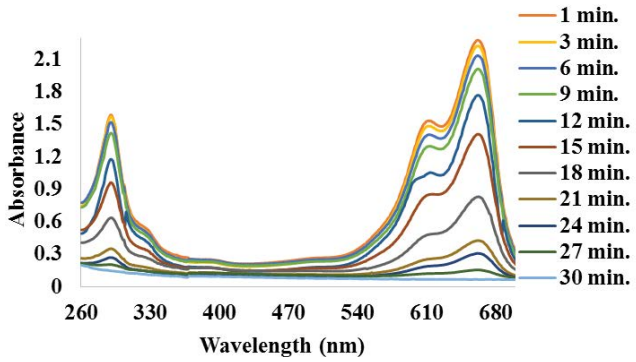

Fig. 5. UV-Vis spectra of methylene blue reduction using MgO-NPs as catalyst.

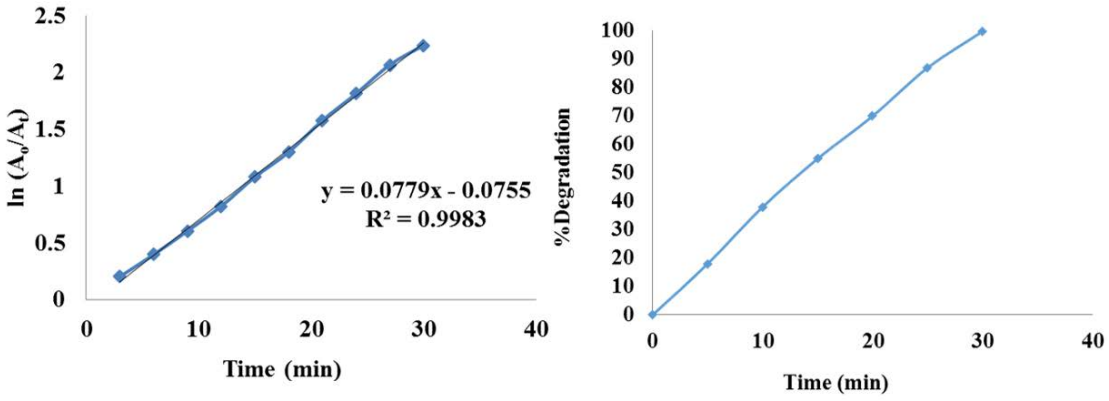

Fig. 6. (a) Kinetic study for degradation of methylene blue dye and (b) percentage degradation for photocatalysis of methylene blue dye.

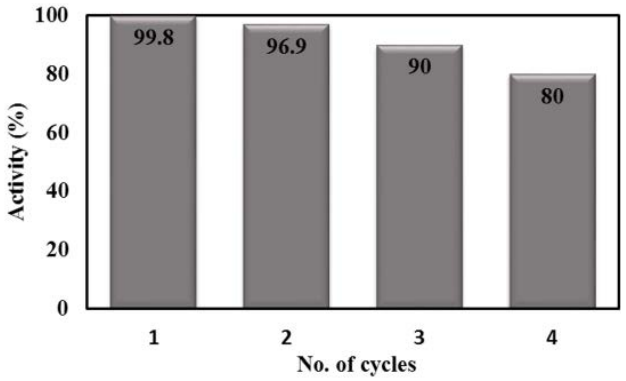

Fig. 7. Percentage recyclability of MgO-NPs.

$$\text{Activity}(\%) = \left(\frac{k_{\text{app}}(n)}{k_{\text{app}}(1)}\right) \times 100 \quad (5)$$

The MgO-NPs catalyst showed excellent stability while a small decrease in catalytic yield was observed. Fig. 7 illustrates that the catalyst showed excellent performance even after 5 cycles. The MgO-NPs showed slight decrease in reduction of MB dye even after five cycles. However, the slight decrease in catalytic performance was observed due to loss of MgO-NPs catalyst during washing and drying process.

4. Conclusion

Low-cost and environmentally friendly methods were used to produce MgO-NPs using *C. gigantea* (Aak plant) root extract. The root extract of Aak plant was used as a capping cum shape-directing agent to regulate the morphology and size of the nanoparticles. The synthesized MgO-NPs were successful in mitigating the environmental pollutant MB dye. Also, MgO-NPs were found to degrade at a rate of 97%. These results indicate that MgO-NPs assembled in a sustainable manner have the potential to be used for the removal of toxic organic pollutants, such as MB dye, from industrial effluents.

Funding

No funds, grants or other support was received.

Conflict of interest

The authors declare no competing interests.

References

[1] V. Anto Feradrick Samson, K. Mohamed Racik, S. Prathap, J. Madhavan, M. Victor Antony Raj, Investigations of structural, optical and dielectric studies of copper oxide nanoparticles, Mater. Today Proc., 8 (2019) 386–392.
[2] S.E. Arasi, M.V.A. Raj, J. Madhavan, Impact of dysprosium (Dy^{3+}) doping on size, optical and dielectric properties of titanium dioxide nanoparticles grown by low temperature hydrothermal method, J. Mater. Sci.: Mater. Electron., 29 (2018) 3170–3177.
[3] Q.M. Jebur, A. Hashim, M.A. Habeeb, Structural, electrical and optical properties for (polyvinyl alcohol–polyethylene oxide–magnesium oxide) nanocomposites for optoelectronics applications, Trans. Electr. Electron. Mater., 20 (2019) 334–343.
[4] M.I. Khan, M.N. Akhtar, N. Ashraf, J. Najeeb, H. Munir, T.I. Awan, M.B. Tahir, M.R. Kabli, Green synthesis of magnesium oxide nanoparticles using *Dalbergia sissoo* extract for photocatalytic activity and antibacterial efficacy, Appl. Nanosci., 10 (2020) 2351–2364.
[5] G. Balducci, L.B. Diaz, D.H. Gregory, Recent progress in the synthesis of nanostructured magnesium hydroxide, Cryst. Eng. Commun., 19 (2017) 6067–6084.
[6] K.D. Khalil, A.H. Bashal, M. Khalafalla, A.A. Zaki, Synthesis, structural, dielectric and optical properties of chitosan-MgO nanocomposite, J. Taibah Univ. Sci., 14 (2020) 975–983.
[7] M. Bindhu, M. Umadevi, M.K. Micheal, M.V. Arasu, N.A. Al-Dhabi, Structural, morphological and optical properties of MgO nanoparticles for antibacterial applications, Mater. Lett., 166 (2016) 19–22.
[8] B.M. Choudary, R.S. Mulukutla, K.J. Klabunde, Benzylation of aromatic compounds with different crystallites of MgO, J. Am. Chem. Soc., 125 (2003) 2020–2021.
[9] H.-L. Shuai, K.-J. Huang, W.-J. Zhang, X. Cao, M.-P. Jia, Sandwich-type microRNA biosensor based on magnesium oxide nanoflower and graphene oxide–gold nanoparticles hybrids coupling with enzyme signal amplification, Sens. Actuators, B, 243 (2017) 403–411.
[10] A. Shahsavar, S. Khanmohammadi, A. Karimipour, M. Goodarzi, A novel comprehensive experimental study concerned synthesizes and prepare liquid paraffin-Fe_3O_4 mixture to develop models for both thermal conductivity & viscosity: a new approach of GMDH type of neural network, Int. J. Heat Mass Transfer, 131 (2019) 432–441.
[11] Z.-X. Tang, B.-F. Lv, MgO nanoparticles as antibacterial agent: preparation and activity, Braz. J. Chem. Eng., 31 (2014) 591–601.
[12] M. Tlili, C. Nefzi, B. Alhalaili, C. Bouzidi, L. Ajili, N. Jebari, R. Vidu, N. Turki Kamoun, Synthesis and characterization of MgO thin films obtained by spray technique for optoelectronic applications, Nanomaterials, 11 (2021) 3076, doi: 10.3390/nano11113076.
[13] S.E.-D. Hassan, A. Fouda, E. Saied, M. Farag, A.M. Eid, M.G. Barghoth, M.A. Awad, M.F. Hamza, M.F. Awad, *Rhizopus oryzae*-mediated green synthesis of magnesium oxide nanoparticles (MgO-NPs): a promising tool for antimicrobial, mosquitocidal action, and tanning effluent treatment, J. Fungi, 7 (2021) 372, doi: 10.3390/jof7050372.
[14] F. Mahmoudi, F. Mahmoudi, K.H. Gollo, M.M. Amini, Biosynthesis of novel silver nanoparticles using *Eryngium thyrsoideum Boiss* extract and comparison of their antidiabetic activity with chemical synthesized silver nanoparticles in diabetic rats, Biol. Trace Elem. Res., 199 (2021) 1967–1978.
[15] A.A. Alrashed, O.A. Akbari, A. Heydari, D. Toghraie, M. Zarringhalam, G.A.S. Shabani, A.R. Seifi, M. Goodarzi, The numerical modeling of water/FMWCNT nanofluid flow and heat transfer in a backward-facing contracting channel, Phys. B: Condens., 537 (2018) 176–183.
[16] N. Rajput, Methods of preparation of nanoparticles – a review, Int. J. Adv. Eng. Technol., 7 (2015) 1806–1811.
[17] A. Tavakoli, M. Sohrabi, A. Kargari, A review of methods for synthesis of nanostructured metals with emphasis on iron compounds, Chem. Pap., 61 (2007) 151–170.
[18] J.-S. Park, W.-H. Chung, H.-S. Kim, Y.-B. Kim, Rapid fabrication of chemical-solution-deposited $La_{0.6}Sr_{0.4}CoO_{3-\delta}$ thin films via flashlight sintering, J. Alloys Compd., 696 (2017) 102–108.
[19] C. Dupas, M. Lahmani, Nanoscience: Nanotechnologies and Nanophysics, Springer Science & Business Media, 2007.
[20] T.H.Y. Duong, T.N. Nguyen, H.T. Oanh, T.A. Dang Thi, L.N.T. Giang, H.T. Phuong, N.T. Anh, B.M. Nguyen, V. Tran Quang, G.T. Le, T.V. Nguyen, Synthesis of magnesium oxide nanoplates and their application in nitrogen dioxide and sulfur dioxide adsorption, J. Chem., 2019 (2019) 4376429, doi: 10.1155/2019/4376429.

[21] P.G. Jamkhande, N.W. Ghule, A.H. Bamer, M.G. Kalaskar, Metal nanoparticles synthesis: an overview on methods of preparation, advantages and disadvantages, and applications, J. Drug Delivery Sci. Technol., 53 (2019) 101174, doi: 10.1016/j.jddst.2019.101174.
[22] H. Pedersen, S.D. Elliott, Studying chemical vapor deposition processes with theoretical chemistry, Theor. Chem. Acc., 133 (2014) 1–10.
[23] J. Hasnidawani, H. Azlina, H. Norita, N. Bonnia, S. Ratim, E. Ali, Synthesis of ZnO nanostructures using sol-gel method, Procedia Chem., 19 (2016) 211–216.
[24] S. Landage, A. Wasif, P. Dhuppe, Synthesis of nanosilver using chemical reduction methods, Int. J. Adv. Eng. Appl. Sci., 3 (2014) 14–22.
[25] A. Karimipour, S.A. Bagherzadeh, M. Goodarzi, A.A. Alnaqi, M. Bahiraei, M.R. Safaei, M.S. Shadloo, Synthesized $CuFe_2O_4$/SiO_2 nanocomposites added to water/EG: evaluation of the thermophysical properties beside sensitivity analysis & EANN, Int. J. Heat Mass Transfer, 127 (2018) 1169–1179.
[26] K. Gudikandula, S. Charya Maringanti, Synthesis of silver nanoparticles by chemical and biological methods and their antimicrobial properties, J. Exp. Nanosci., 11 (2016) 714–721.
[27] J. Singh, T. Dutta, K.-H. Kim, M. Rawat, P. Samddar, P. Kumar, 'Green' synthesis of metals and their oxide nanoparticles: applications for environmental remediation, J. Nanobiotechnol., 16 (2018) 1–24.
[28] M.L. Guimarães, F.A.G. da Silva, M.M. da Costa, H.P. de Oliveira, Green synthesis of silver nanoparticles using *Ziziphus joazeiro* leaf extract for production of antibacterial agents, Appl. Nanosci., 10 (2020) 1073–1081.
[29] M. Ovais, A.T. Khalil, A. Raza, N.U. Islam, M. Ayaz, M. Saravanan, M. Ali, I. Ahmad, M. Shahid, Z.K. Shinwari, Multifunctional theranostic applications of biocompatible green-synthesized colloidal nanoparticles, Appl. Microbiol. Biotechnol., 102 (2018) 4393–4408.
[30] M. Ayaz, M. Junaid, F. Ullah, F. Subhan, A. Sadiq, G. Ali, M. Ovais, M. Shahid, A. Ahmad, A. Wadood, Anti-Alzheimer's studies on β-sitosterol isolated from *Polygonum hydropiper* L, Front. Pharmacol., 8 (2017) 697, doi: 10.3389/fphar.2017.00697.
[31] V. Makarov, A. Love, O. Sinitsyna, S. Makarova, I. Yaminsky, M. Taliansky, N. Kalinina, "Green" nanotechnologies: synthesis of metal nanoparticles using plants, Acta Nat., 6 (2014) 35–44.
[32] S.P. Fernández, C. Wasowski, L.M. Loscalzo, R.E. Granger, G.A. Johnston, A.C. Paladini, M. Marder, Central nervous system depressant action of flavonoid glycosides, Eur. J. Pharmacol., 539 (2006) 168–176.
[33] Y. Abdallah, S.O. Ogunyemi, A. Abdelazez, M. Zhang, X. Hong, E. Ibrahim, A. Hossain, H. Fouad, B. Li, J. Chen, The green synthesis of MgO nano-flowers using *Rosmarinus officinalis* L. (Rosemary) and the antibacterial activities against *Xanthomonas oryzae* pv. *oryzae*, Biomed Res. Int., 2019 (2019) 5620989, doi: 10.1155/2019/5620989.
[34] S.O. Ogunyemi, F. Zhang, Y. Abdallah, M. Zhang, Y. Wang, G. Sun, W. Qiu, B. Li, Biosynthesis and characterization of magnesium oxide and manganese dioxide nanoparticles using *Matricaria chamomilla* L. extract and its inhibitory effect on *Acidovorax oryzae* strain RS-2, Artif. Cells Nanomed. Biotechnol., 47 (2019) 2230–2239.
[35] G. Parihar, N. Balekar, *Calotropis procera*: a phytochemical and pharmacological review, Thai J. Pharm. Sci., 40 (2016) 115–131.
[36] A. Mushir, N. Jahan, A. Ahmed, A review on phytochemical and biological properties of *Calotropis gigantea* (Linn.) R.Br, Dis. Phytomed., 3 (2016) 15.
[37] M.A. Al Sulaibi, C. Thiemann, T. Thiemann, Chemical constituents and uses of *Calotropis procera* and *Calotropis gigantea* – a review (Part I – the plants as material and energy resources), Open Chem. J., 8 (2020) 1–15.
[38] P.K. Pattnaik, D. Kar, H. Chhatoi, S. Shahbazi, G. Ghosh, A. Kuanar, Chemometric profile & antimicrobial activities of leaf extract of *Calotropis procera* and *Calotropis gigantea*, Nat. Prod. Res., 31 (2017) 1954–1957.
[39] M.O. Barbosa, J.S. de Almeida-Cortez, S.I. da Silva, A.F.M. de Oliveira, Seed oil content and fatty acid composition from different populations of *Calotropis procera* (Aiton) WT Aiton (*Apocynaceae*), J. Am. Oil Chem. Soc., 91 (2014) 1433–1441.
[40] B.D. Wadhwani, D. Mali, P. Vyas, R. Nair, P. Khandelwal, A review on phytochemical constituents and pharmacological potential of *Calotropis procera*, RSC Adv., 11 (2021) 35854–35878.
[41] R. Gyawali, B. Bhattarai, S. Bajracharya, S. Bhandari, P. Bhetwal, K. Bogati, S. Neupane, S. Shrestha, A.K. Shrestha, R. Joshi, α-amylase inhibition, antioxidant activity and phytochemical analysis of *Calotropis gigantea* (L.) Dryand, J. Allied Health Sci., 10 (2020) 77–81.
[42] M.I. Din, A.G. Nabi, A. Rani, A. Aihetasham, M. Mukhtar, Single step green synthesis of stable nickel and nickel oxide nanoparticles from *Calotropis gigantea*: catalytic and antimicrobial potentials, Environ. Nanotechnol. Monit. Manage., 9 (2018) 29–36.
[43] R. Dobrucka, Synthesis of MgO nanoparticles using *Artemisia abrotanum* herba extract and their antioxidant and photocatalytic properties, Iran. J. Sci. Technol. Trans. A: Sci., 42 (2018) 547–555.
[44] L. Gharibshahi, E. Saion, E. Gharibshahi, A.H. Shaari, K.A. Matori, Structural and optical properties of Ag nanoparticles synthesized by thermal treatment method, Materials (Basel), 10 (2017) 402, doi: 10.3390/ma10040402.
[45] Z.-X. Tang, X.-J. Fang, Z.-L. Zhang, T. Zhou, X.-Y. Zhang, L.-E. Shi, Nanosize MgO as antibacterial agent: preparation and characteristics, Braz. J. Chem. Eng., 29 (2012) 775–781.
[46] A. Almontasser, A. Parveen, A. Azam, Synthesis, characterization and antibacterial activity of magnesium oxide (MgO) nanoparticles, IOP Conf. Ser.: Mater. Sci. Eng., 577 (2019) 012051, doi: 10.1088/1757-899X/577/1/012051.
[47] A. Pugazhendhi, R. Prabhu, K. Muruganantham, R. Shanmuganathan, S. Natarajan, Anticancer, antimicrobial and photocatalytic activities of green synthesized magnesium oxide nanoparticles (MgONPs) using aqueous extract of *Sargassum wightii*, J. Photochem. Photobiol., B, 190 (2019) 86–97.
[48] A. Fouda, S.E.-D. Hassan, E. Saied, M.F. Hamza, Photocatalytic degradation of real textile and tannery effluent using biosynthesized magnesium oxide nanoparticles (MgO-NPs), heavy metal adsorption, phytotoxicity, and antimicrobial activity, J. Environ. Chem. Eng., 9 (2021) 105346, doi: 10.1016/j.jece.2021.105346.
[49] J. Suresh, R. Yuvakkumar, M. Sundrarajan, S.I. Hong, Green synthesis of magnesium oxide nanoparticles, Adv. Mater. Res., 952 (2014) 141–144.
[50] M.I. Din, R. Khalid, Z. Hussain, Novel *in-situ* synthesis of copper oxide nanoparticle in smart polymer microgel for catalytic reduction of methylene blue, J. Mol. Liq., 358 (2022) 119181, doi: 10.1016/j.molliq.2022.119181.
[51] G. Liao, W. Zhao, Q. Li, Q. Pang, Z. Xu, Novel poly(acrylic acid)-modified tourmaline/silver composites for adsorption removal of Cu(II) ions and catalytic reduction of methylene blue in water, Chem. Lett., 46 (2017) 1631–1634.
[52] B.A. Abdulkadir, A. Ramli, L.J. Wei, Y. Uemura, Effect of MgO Loading on the production of biodiesel from Jatropha oil in the presence of MgO/MCM-22 Catalyst, J. Jpn. Inst. Eng., 97 (2018) 191–199.